

Advanced analysis of uncertain cracked structures

P. Bocchini, C. Gentilini, F. Ubertini and E. Viola ¹

Abstract: This paper provides a simple and reliable method for the probabilistic characterization of the linear elastic response of frame structures with edge cracks of uncertain depth and location. A statistical analysis of the structural response allows consideration of the reliability of the investigated structure. A numerical example provides an indication of the performance of the approach proposed.

keyword: Cracked beam, Uncertain damage, Reliability, Probability distribution fitting, Skew-Normal distribution.

1 Introduction

For a realistic description of the structural behavior of cracked structures, crack depth and crack location should be defined in a probabilistic sense and modelled as uncertain parameters. In the literature, the most common procedures for the stochastic analysis of structures with uncertain parameters are Monte Carlo simulation (see, for example, the survey paper by Hurtado and Barbat, 1998) and perturbation techniques (see, for example, the survey paper by Matthies, Brenner, Bucher, and Soares, 1997). The main drawbacks of these approaches are, for the former, the high computational cost involved to obtain statistical convergence and, for the latter, the low accuracy as the level of uncertainty increases. Based on the above remarks, a computationally efficient and accurate method has been presented by Di Paola (2004) to analyse truss structures with uncertain geometrical and mechanical properties. This approach has been generalized for the probabilistic analysis of linear elastic edge-cracked truss and frame structures with uncertain crack features in Gentilini, Ubertini, and Viola (2005a).

Here, the stochastic method is applied to multicracked frame structures aiming at assessing the overall reliabil-

ity. The crack is modelled by introducing a local compliance that produces a discontinuity of displacements in correspondence with the cracked section (Okamura, Watanabe, and Takano, 1975). The local compliance due to the presence of the crack depends on the crack depth and location and it is obtained via energy balance between the external work and fracture work. This leads to the known relationships between the additional compliance contributions due to the crack and the stress intensity factors (Muller, Herrmann, and Gao, 1993). Finally, the compliance matrix of the cracked member is obtained by simply adding the compliance matrix of the intact element to the overall compliance due to the crack. The uncertainties affecting cracks are transformed into superimposed strains on a deterministic equivalent structure. For redundant structures, an asymptotic series expansion is obtained. Numerical results show that few terms of the series are enough to accurately characterize the structural response (Gentilini, Viola, and Ubertini, 2003; Gentilini, Ubertini, and Viola, 2005b).

The results of the stochastic analysis are then used for reliability-oriented evaluations. For example, designers can be interested in the probability to reach a certain “limit state” or in the value of a particular variable of the structural response that is overcome only in the *n-per-cent* of the cases. Both problems reduce to the computation of quantiles of the random variables that characterize the structural response. This task can be carried out by evaluating quantiles directly on the samples computed by the proposed stochastic method. However, a more comprehensive statistical survey can lead to a better overall description.

Kernel smoothing techniques (Bowman and Azzalini, 1997) provide a smoothed “empirical” probability density function (PDF) that, to a first approximation, can be assumed as the PDF of the population. In this way the values of quantiles are influenced by the complete shape of the sample distribution. Moreover, these techniques avoid the rough PDF curves that are obtained whenever the number of bins of the frequency histogram is too large

¹ DISTART, University of Bologna, Italy. Some results have been presented at the fourth International Conference on Fracture and Damage Mechanics (12-14 July 2005, Mallorca, Spain), see Gentilini, Ubertini, and Viola (2005b)

(see, for example, Benjamin and Cornell, 1970, chap. 1). If a complete description of the distribution is required, neither the relative frequency histogram, nor the smoothed PDF are sufficient. In this case the solution is to fit an appropriate theoretical probability distribution. If there is *a priori* information on the expected shape of the PDF, the attention can be focused on a specific family of probability distributions. In practical structural problems, this information is, in general, unavailable. Thus, in the following, tools that overcome this deficiency are suggested. In particular, three-parameter distributions are considered, because they can change their location, their scale, and also their shape. Bocchini, Ubertini, and Viola (2005) have proposed an iterative method for the fitting of a three-parameter Weibull distribution in the structural framework. This procedure is able to work even in conjunction with stochastic methods that compute only descriptive statistics of the structural response. Otherwise, if a complete sample of the response is available, as in the case presented in this paper, other techniques can fit probability distributions even better. One of the most versatile class of methods is the minimization of a “distance” between empirical samples and theoretical distributions. The well-known maximum likelihood method (MLE) belongs to this class. A different distance, that is more suitable for use by engineers, has been proposed by Chou, Ingram, and Corotis (2005). In particular, they have suggested to use the index D_{KS} of the Kolmogorov-Smirnov hypothesis test (Benjamin and Cornell, 1970, chap. 4) that represents the maximum distance between the empirical and theoretical Cumulative Distribution Functions (CDFs). Therefore, from our point of view, it is interesting because it minimizes the difference from theoretical and empirical quantiles.

A critical comparison between the results obtained by the above mentioned data treatments have been performed aiming at evaluating the effectiveness and versatility of a reliability analysis based on the presented stochastic approach.

2 Stochastic analysis

Attention is focused on the linear elastic Timoshenko beam element represented in Fig. 1. In the hypothesis of absence of distributed loads, the response of the beam element is governed by the following equations:

$$\mathbf{e}_a = \mathbf{D}_a \mathbf{u}_a \quad (1)$$

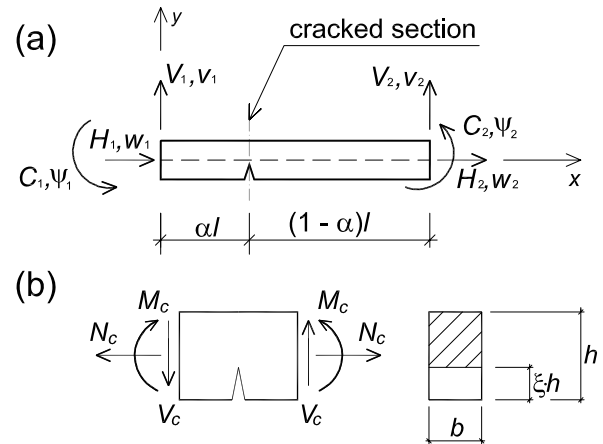


Figure 1 : Cracked (a) beam element and (b) section

$$\mathbf{D}_a^T \mathbf{q}_a = \mathbf{S}_a \quad (2)$$

$$\mathbf{e}_a = \mathbf{C}_a \mathbf{q}_a \quad (3)$$

where \mathbf{u}_a is the vector of nodal displacements, \mathbf{S}_a is the vector of nodal forces, \mathbf{D}_a and \mathbf{D}_a^T are the compatibility and equilibrium matrices and \mathbf{C}_a is the compliance matrix. The vector of natural deformations is $\mathbf{e}_a = [e \ \varphi_s \ \varphi_{as}]^T$ and the corresponding natural internal force vector is $\mathbf{q}_a = [N \ C_s \ C_{as}]^T$ as proposed by Argyris, Balmer, Doltsinis, Dunne, Haase, Kleiber, Malejannakis, Mlejnek, Müller, and Scharpf (1979). Thus, the compatibility matrix takes the form

$$\mathbf{D}_a = \begin{bmatrix} -1 & 0 & 0 & 1 & 0 & 0 \\ 0 & 0 & -1 & 0 & 0 & 1 \\ 0 & -2/l & -1 & 0 & 2/l & -1 \end{bmatrix} \quad (4)$$

being l the length of the beam. Let assume that the beam is affected by uncertainties, which influence the compliance matrix:

$$\mathbf{C}_a = \mathbf{C}_a(\beta_a) \quad (5)$$

where β_a is a vector of uncertain parameters modelled as random variables. In this paper crack depth and location are modelled as uncertain parameters. To evaluate the structural response, natural internal forces are expressed in terms of nodal displacements

$$\mathbf{q}_a = \mathbf{G}_a(\beta_a) \mathbf{u}_a \quad (6)$$

and the classical relation between nodal forces and nodal displacements is obtained

$$\mathbf{S}_a = \mathbf{K}_a(\beta_a) \mathbf{u}_a \quad (7)$$

where $\mathbf{G}_a(\beta_a) = \mathbf{C}_a^{-1}(\beta_a)\mathbf{D}_a$ and $\mathbf{K}_a(\beta_a) = \mathbf{D}_a^T \mathbf{C}_a^{-1}(\beta_a)\mathbf{D}_a$. Then, according to the standard matrix assembly procedure, the equilibrium equation for the whole structure is obtained

$$\mathbf{K}(\beta)\mathbf{u} = \mathbf{F} \quad (8)$$

where $\mathbf{K}(\beta)$ is the (stochastic) structure stiffness matrix, \mathbf{u} is the vector of unknown nodal displacements, \mathbf{F} is the vector of prescribed nodal forces and β is a random vector collecting variables β_a . Natural internal forces \mathbf{q} can be derived from nodal displacements by the relation

$$\mathbf{q} = \mathbf{G}(\beta)\mathbf{u} \quad (9)$$

where \mathbf{q} collects vectors \mathbf{q}_a and \mathbf{G} is obtained from the assemblage of \mathbf{G}_a . To characterize the structural response, nodal displacements should be evaluated as functions of the random variables β by solving Eq. (8). In the literature, much effort has been directed towards developing approximate approaches. Here, the stochastic approach presented by Gentilini, Ubertini, and Viola (2005a) is followed.

2.1 The method: formulation and solution procedure

The basic idea is to split the element compliance matrix into a deterministic part \mathbf{C}_a^0 and an additional part \mathbf{C}_a^β affected by uncertainty

$$\mathbf{C}_a(\beta_a) = \mathbf{C}_a^0 + \mathbf{C}_a^\beta(\beta_a) \quad (10)$$

From here onward, superscript 0 is used for deterministic quantities, while superscript β for random quantities. With the above assumption, Eq. (3) can be put in the form

$$\mathbf{e}_a = \mathbf{C}_a^0 \mathbf{q}_a + \mathbf{e}_a^\beta \quad (11)$$

where

$$\mathbf{e}_a^\beta = \mathbf{C}_a^\beta \mathbf{q}_a \quad (12)$$

are called virtual superimposed strains, because they originate from the presence of uncertainties. In other words, the effect of uncertainties is taken into account through superimposed strains \mathbf{e}_a^β . Based on this observation, the element equations (6) and (7) are rewritten in the new form

$$\mathbf{q}_a = \mathbf{G}_a^0 \mathbf{u}_a + \mathbf{R}_a^\beta \quad \mathbf{S}_a = \mathbf{K}_a^0 \mathbf{u}_a - \mathbf{F}_a^\beta \quad (13)$$

where $\mathbf{G}_a^0 = (\mathbf{C}_a^0)^{-1} \mathbf{D}_a$, $\mathbf{K}_a^0 = \mathbf{D}_a^T (\mathbf{C}_a^0)^{-1} \mathbf{D}_a$, $\mathbf{R}_a^\beta = -(\mathbf{C}_a^0)^{-1} \mathbf{e}_a^\beta$ and $\mathbf{F}_a^\beta = \mathbf{D}_a^T \mathbf{R}_a^\beta$. In this framework, \mathbf{R}_a^β can be interpreted as the stress vector induced by the virtual superimposed strains \mathbf{e}_a^β which depends on the actual stress distribution. In fact, through Eq. (12), it is possible to obtain

$$\mathbf{R}_a^\beta = \mathbf{L}_a^\beta \mathbf{q}_a \quad \mathbf{F}_a^\beta = -\mathbf{D}_a^T \mathbf{L}_a^\beta \mathbf{q}_a \quad (14)$$

with matrix $\mathbf{L}_a^\beta = -(\mathbf{C}_a^0)^{-1} \mathbf{C}_a^\beta$ that embodies all the uncertainties. Starting from the above equations, the standard procedure of assemblage and enforcement of displacement boundary conditions leads to the new format of the governing equations for the entire structure

$$\mathbf{K}^0 \mathbf{u} = \mathbf{F} + \mathbf{F}^\beta \quad \mathbf{q} = \mathbf{G}^0 \mathbf{u} + \mathbf{R}^\beta \quad (15)$$

where $\mathbf{R}^\beta = \mathbf{L}^\beta \mathbf{q}$ and $\mathbf{F}^\beta = -\mathbf{D}^T \mathbf{L}^\beta \mathbf{q}$.

In the linear elastic framework, Eq. (15) leads naturally to a subdivision of the structure into two systems, see Fig. 2. The first system is a (reference) deterministic structure subjected to the prescribed loads \mathbf{F} and ruled by the equations

$$\mathbf{K}^0 \mathbf{u}^0 = \mathbf{F} \quad \mathbf{q}^0 = \mathbf{G}^0 \mathbf{u}^0 \quad (16)$$

that can be easily solved in \mathbf{u}^0 and \mathbf{q}^0 by means of standard procedures. The second (auxiliary) system is the same deterministic structure but subjected to \mathbf{F}^β instead of \mathbf{F}

$$\mathbf{K}^0 \mathbf{u}^\beta = \mathbf{F}^\beta \quad \mathbf{q}^\beta = \mathbf{G}^0 \mathbf{u}^\beta + \mathbf{R}^\beta \quad (17)$$

Thus, by means of the superposition principle, the expressions of \mathbf{u} and \mathbf{q} for the original structure take the form

$$\mathbf{u} = \mathbf{u}^0 + \mathbf{u}^\beta \quad \mathbf{q} = \mathbf{q}^0 + \mathbf{q}^\beta \quad (18)$$

It is worthy to remark that the two systems differ only for the load condition. In particular, only the second system is affected by uncertainties, which enter as nodal loads equivalent to the virtual superimposed strains. Solving the original problem reduces to solve Eq. (17). However, this is not trivial because \mathbf{F}^β depends on the yet unknown stress distribution. In particular, using Eq. (17) the following relations can be obtained:

$$\mathbf{u}^\beta = \mathbf{U} \mathbf{L}^\beta \mathbf{q} \quad \mathbf{q}^\beta = \mathbf{W} \mathbf{L}^\beta \mathbf{q} \quad (19)$$

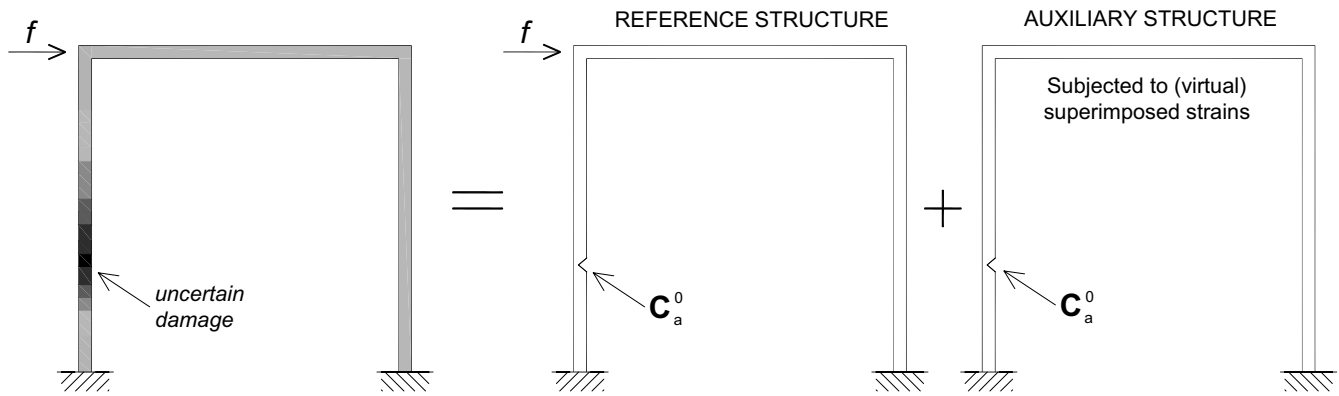


Figure 2 : Cracked frame structure with uncertain damage: superposition principle.

where $\mathbf{U} = -(\mathbf{K}^0)^{-1} \mathbf{D}^T$ and $\mathbf{W} = \mathbf{I} + \mathbf{G}^0 \mathbf{U}$. Hence it is appropriate to establish a recurrence relation that finally leads to the following expansion for the stress vector \mathbf{q} and displacement vector \mathbf{u} of the original structure:

$$\mathbf{q} = \left[\sum_{j=0}^{\infty} (\mathbf{W} \mathbf{L}^\beta)^j \right] \mathbf{q}^0 \quad (20)$$

$$\mathbf{u} = \mathbf{u}^0 + \mathbf{U} \mathbf{L}^\beta \left[\sum_{j=0}^{\infty} (\mathbf{W} \mathbf{L}^\beta)^j \right] \mathbf{q}^0 \quad (21)$$

Notice that in the case of statically determinate structures the solution is simply given by

$$\mathbf{q} = \mathbf{q}^0 \quad \mathbf{u} = \mathbf{u}^0 + \mathbf{U} \mathbf{L}^\beta \mathbf{q}^0 \quad (22)$$

The probabilistic characterization of the response can be made by following two different strategies: (i) analytical evaluation of the statistical moments of the response starting from Eq. (21) (some useful expressions are given by Di Paola, 2004) or (ii) application of Monte Carlo simulation to Eq. (21). It can be easily realized that such a simulation is, anyway, enormously more efficient than a simulation applied directly to the governing equations.

Notice that the series expansion in Eq. (21) converges to the solution of the original problem if some attention is paid to select the deterministic compliances \mathbf{C}_a^0 , which actually characterize the reference deterministic structure. It can be demonstrated that the resultant element-wise sufficient condition for convergence can be written as

$$\rho^U < 1 \quad \rho^U = \max_{\beta_a \in \mathcal{B}_a} \rho(\mathbf{L}_a^\beta) \quad (23)$$

that results in the following optimal choice for \mathbf{C}_a^0 :

$$\mathbf{C}_a^0 \in \text{Sym}^+ \quad \text{such that} \quad \rho^U = \text{minimum} \quad (24)$$

where ρ^U is the spectral radius of \mathbf{L}_a^β and \mathcal{B}_a is the range of β_a . Based on this choice, a globally optimal convergence rate is expected. More details about the convergence analysis of the series can be found in Gentilini, Ubertini, and Viola (2005a).

2.2 Cracked beam with uncertain damage

Consider the edge-cracked beam shown in Fig. 1. In correspondence of the cracked zone, the axial force N_c causes an additional angular deformation, together with an additional elongation, as well as the bending moment M_c causes an additional elongation together with an additional angular deformation. Moreover, the shear force V_c causes an additional deflection. This can be modelled by suitably defining local compliance contributions due to the crack

$$\left[\Delta w_c \quad \Delta \theta_c \quad \Delta v_c \right]^T = \widehat{\mathbf{C}}_a^{crack} \left[N_c \quad M_c \quad V_c \right]^T$$

with Δw_c total additional elongation, $\Delta \theta_c$ total angular deformation, Δv_c total additional deflection and

$$\widehat{\mathbf{C}}_a^{crack} = \begin{bmatrix} \lambda_N & \lambda_{NM} & 0 \\ \lambda_{NM} & \lambda_M & 0 \\ 0 & 0 & \lambda_V \end{bmatrix} \quad (25)$$

To compute the overall compliance of the cracked element, the additional deformations and the stress resultants at the cracked section should be expressed in terms of the natural deformations and internal forces

$$\left[N_c \quad M_c \quad V_c \right]^T = \mathbf{T} \left[N \quad C_s \quad C_{as} \right]^T$$

$$\left[e \quad \varphi_s \quad \varphi_{as} \right]_{crack}^T = \mathbf{T}^T \left[\Delta w_c \quad \Delta \theta_c \quad \Delta v_c \right]^T$$

where the transformation matrix \mathbf{T} depends on the dimensionless crack location α (see Fig. 1) and reads as

$$\mathbf{T} = \begin{bmatrix} 1 & 0 & 0 \\ 0 & 1 & 1-2\alpha \\ 0 & 0 & 2/l \end{bmatrix} \quad (26)$$

Then, the overall additional compliance due to the crack is given by

$$\mathbf{C}_a^{crack}(\xi, \alpha) = \mathbf{T}^T(\alpha) \widehat{\mathbf{C}}_a^{crack}(\xi) \mathbf{T}(\alpha) \quad (27)$$

where ξ is the dimensionless crack depth. Finally, the compliance matrix of the cracked beam is simply obtained by

$$\mathbf{C}_a = \mathbf{C}_a^{in} + \mathbf{C}_a^{crack} \quad (28)$$

where \mathbf{C}_a^{in} is the compliance matrix for an intact, homogeneous beam with constant cross-section

$$\mathbf{C}_a^{in} = \begin{bmatrix} l/E\mathcal{A} & 0 & 0 \\ 0 & l/EJ & 0 \\ 0 & 0 & l(1+\kappa_s)/3EJ \end{bmatrix} \quad (29)$$

with $\kappa_s = 12EJ/(G\mathcal{A}_s l^2)$, E the Young's modulus, G the shear modulus, \mathcal{A} the cross-section area, J the inertia moment and \mathcal{A}_s the shear area. The local compliance contributions attributable to the crack can be determined by the well-known relationship among energy release rate, stress intensity factors and compliance (Okamura, Watanabe, and Takano, 1975)

$$\lambda_N = \frac{2(1-\nu^2)}{E} \int_0^{\mathcal{A}_{crack}} \left(\frac{K_{IN}}{N} \right)^2 d\mathcal{A}_{crack} \quad (30)$$

$$\lambda_M = \frac{2(1-\nu^2)}{E} \int_0^{\mathcal{A}_{crack}} \left(\frac{K_{IM}}{M} \right)^2 d\mathcal{A}_{crack} \quad (31)$$

$$\lambda_{NM} = \frac{2(1-\nu^2)}{E} \int_0^{\mathcal{A}_{crack}} \frac{K_{IN}}{N} \frac{K_{IM}}{M} d\mathcal{A}_{crack} \quad (32)$$

$$\lambda_V = \frac{2(1-\nu^2)}{E} \int_0^{\mathcal{A}_{crack}} \left(\frac{K_{II}}{V} \right)^2 d\mathcal{A}_{crack} \quad (33)$$

where K_{IN} and K_{IM} are the Mode I stress intensity factors caused by the axial force and bending moment,

respectively, and K_{II} is the Mode II stress intensity factor caused by the shear force, \mathcal{A}_{crack} is the cracked area and ν is the Poisson's ratio for plane strain and zero for plane stress. In order to apply the above equations, the stress intensity factors for the current structural configuration can be often found in handbooks (see, for example, Murakami, 1987) or, otherwise, determined by various analytical and numerical approaches (see, for example, Nobile, 2000; Muller, Herrmann, and Gao, 1993). For a $b \times h$ rectangular cross-section with an edge crack (see Fig. 1) the stress intensity factors can be put in the form

$$K_{IN} = \frac{N}{bh} \sqrt{\pi\xi} h F_N(\xi) \quad (34)$$

$$K_{IM} = \frac{6M^2}{bh} \sqrt{\pi\xi} h F_M(\xi) \quad (35)$$

$$K_{II} = \frac{V}{b} \sqrt{h(1-\xi)} \sqrt{\pi\xi} h F_V(\xi) \quad (36)$$

where the correction functions can be taken as proposed in Tharp (1987): $F_N(\xi) = 1.12 - 0.23\xi + 10.6\xi^2 - 21.7\xi^3 + 30.4\xi^4$, $F_M(\xi) = 1.12 - 1.39\xi + 7.32\xi^2 - 13.1\xi^3 + 14\xi^4$ and $F_V(\xi) = 1.993\xi + 4.513\xi^2 - 9.516\xi^3 + 4.482\xi^4$, with $\xi \leq 0.6$.

The dimensionless crack depth ξ and location α are modelled by random variables with given probabilistic characteristics. Based on the present method of analysis, the cracked beam compliance is rewritten as

$$\mathbf{C}_a(\xi, \alpha) = \mathbf{C}_a^0 + \mathbf{C}_a^\beta(\xi, \alpha) \quad (37)$$

To optimize the convergence rate it is convenient to derive a value for \mathbf{C}_a^0 from the beam compliance for a certain crack depth ξ^0 and location α^0

$$\mathbf{C}_a^0 = \mathbf{C}_a(\xi^0, \alpha^0) \quad (38)$$

In particular, ξ^0 and α^0 are selected based on criterion (24). It should be remarked that the optimal values ξ^0 and α^0 are generally different from the mean values of ξ and α .

3 Reliability analysis

The complete probabilistic characterization of the structural response, obtained by the proposed stochastic method, is used here aiming at computing the probability

to reach a certain limit value or, more generally, evaluating the structural reliability. To this purpose, various statistical approaches, that need different input requirements, can be adopted. The choice among these methods depends on the available data and the objectives of the assessment. Usually, statistical inferences are “parametric inferences”. This means that the response is modelled by assuming a certain parametric family of probability distributions. Actually, in the structural applications, it is very difficult to guess the shape of the distribution of random variables that characterize the response.

In the following, four different approaches are considered. The first approach (Section 3.1) is to compute directly descriptive statistics of the results of the analysis. The second approach (Section 3.2) is to use non-parametric statistics and tools that do not require to introduce a theoretical PDF. The third approach (Section 3.3) is to use versatile parametric PDFs able to adapt also their shape, as the three-parameter distributions. The last approach (Section 3.4) is to fit various families of curves and compare the “goodness of fit” for the data by means of an appropriate metric.

In the numerical application (Section 4) all the above mentioned statistical techniques are applied to the results predicted by the stochastic analysis of a multicracked frame structure in order to assess the structural reliability.

3.1 Rough data analysis

The first approach is to analyse the rough data by computing the relative frequency histograms, such as those represented in Fig. 3(a) and Fig. 3(b), and using them to assess the desired percentiles. Clearly, this is a crude analysis which does not effectively exploit all the available information coming from the structural response. For example, the two (normalized) relative frequency histograms in Fig. 3 have the same 4th, 10th and 20th percentiles (respectively 1.5, 2.5 and 3.5) even if it is evident that the two samples are taken from very different populations. If the computation of the quantiles reduces only to determine the value of the cumulative distribution histogram in one point, its shape is ignored, and most of the available information is wasted. In particular, this often leads to a poor description of the tails of the distribution. This drawback causes an inaccurate computation of the extreme quantiles that are of utmost importance in structural design.

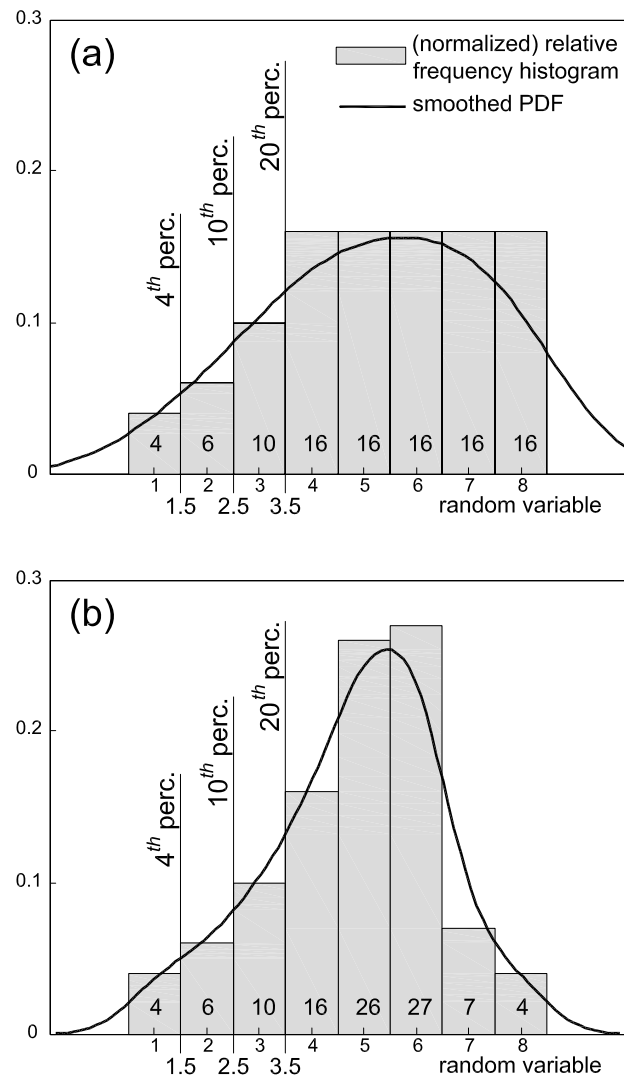


Figure 3 : Normalized relative frequency histograms and smoothed PDFs of two different samples that lead to similar left-tail quantiles (100 elements for each sample).

3.2 Kernel smoothing

A more accurate approach is to apply a smoothing procedure to the rough data obtained by the structural analysis. This non-parametric technique substitutes a smoothed curve for the (normalized) relative frequency histogram, as the continuous lines in Fig. 3(a) and Fig. 3(b). Here, the smoothing takes account of the shape of the probability distribution. The effect is evident especially for the right-tail.

The frequency histogram can be described by

$$\bar{f}(x) = \sum_{i=1}^n I(x - \tilde{x}_i; k) \quad (39)$$

where n is the number of data, x_i are the observed data, \tilde{x}_i are the centers of the intervals in which x_i fall, $2k$ is the bin size and $I(z; k)$ is the indicator function

$$I(z; k) = \begin{cases} 1 & \text{if } z \in [-k, k] \\ 0 & \text{otherwise} \end{cases} \quad (40)$$

Therefore, the normalized histogram is described by

$$\tilde{f}(x) = \frac{1}{2kn} \sum_{i=1}^n I(x - \tilde{x}_i; k) \quad (41)$$

The smoothing techniques replace the indicator function with a continuous function $w(z; k)$, called “kernel function”, centered directly over each observation. If the kernel function has unitary integral, the normalized PDF is

$$\hat{f}(x) = \frac{1}{n} \sum_{i=1}^n w(x - x_i; k) \quad (42)$$

To evaluate the most suitable kernel function and the optimum bandwidth k , different approaches can be adopted (Epanechnikov, 1969; Bowman and Azzalini, 1997). In the numerical example of Section 4 good results have been obtained using a standard gaussian kernel (eventually bounded) and the optimum bandwidth for the resultant PDFs.

3.3 Fitting of three-parameter distributions

An alternative approach is to fit a versatile parametric distribution, such as a three-parameter distribution, to the rough data.

3.3.1 The Type III Extreme Values distribution

A widely used three-parameter distribution is the Type III Extreme Values distribution. In the literature, it is presented in two forms linked by the “symmetry principle” (Ang and Tang, 1984): the “Type III asymptotic distribution of the largest value” and the “Type III asymptotic distribution of the smallest value”, also called “Weibull distribution” and sometimes presented in a special form with only two parameters.

The Weibull distribution with parameters A , B and C that is considered in this work is defined by

$$PDF : f(x) = \frac{C}{B} \left(\frac{x-A}{B} \right)^{C-1} e^{-\left(\frac{x-A}{B}\right)^C} \quad (43)$$

$$CDF : F(x) = 1 - e^{-\left(\frac{x-A}{B}\right)^C}$$

with B and C assumed to be positive, and $x > A$. This distribution describes both symmetric and skew curves with skewness $\gamma \in (-1.14, +\infty)$ for reasonable values of parameter C .

The Type III asymptotic distribution of the largest value with parameters A , B and C is represented by

$$PDF : f(x) = \frac{C}{B} \left(\frac{A-x}{B} \right)^{C-1} e^{-\left(\frac{A-x}{B}\right)^C} \quad (44)$$

$$CDF : F(x) = e^{-\left(\frac{A-x}{B}\right)^C}$$

where B and C are assumed to be positive and A is the upper bound for the domain of x . This distribution describes both symmetric and skew curves with $\gamma \in (-\infty, 1.14)$ for reasonable values of parameter C .

The Weibull distribution presents well-known difficulties in the estimation process. Here, the adopted estimators are the following:

$$\hat{\mu} = \frac{1}{n} \sum_{i=1}^n x_i \quad (45)$$

$$\hat{\sigma}^2 = \frac{1}{n-1} \sum_{i=1}^n (x_i - \hat{\mu})^2 \quad (46)$$

$$\hat{\gamma} = \frac{n \sum_{i=1}^n (x_i - \hat{\mu})^3}{(n-1)(n-2)\hat{\sigma}^3} \quad (47)$$

Mean, variance and skewness of a theoretical Weibull distribution are

$$\mu = A + B\Gamma(C_1) \quad (48)$$

$$\sigma^2 = B^2 [\Gamma(C_2) - \Gamma^2(C_1)] \quad (49)$$

$$\gamma = \frac{2\Gamma^3(C_1) - 3\Gamma(C_1)\Gamma(C_2) + \Gamma(C_3)}{\sqrt{[\Gamma(C_2) - \Gamma^2(C_1)]^3}} \quad (50)$$

where:

$$\Gamma(x) = \int_0^{\infty} t^{x-1} e^{-t} dt \tag{51}$$

$$C_1 = \frac{C+1}{C} \tag{52}$$

$$C_2 = \frac{C+2}{C} \tag{53}$$

$$C_3 = \frac{C+3}{C} \tag{54}$$

The system of equations (48)–(50) can not be analytically solved with respect to the parameters, due to the presence of the Gamma function (51). Therefore a solution based on an iterative scheme is proposed.

It can be noticed that Eq. (50) depends only on parameter C , so the procedure starts by analysing it. The starting value, obtained with a linear regression made on the interval of values where the skewness of samples can be most frequently found, is

$$C^{(1)} = 0.677\hat{\gamma} + 2.7 \tag{55}$$

The relationship between C and the skewness γ is strictly decreasing, as it can be seen by differentiating Eq. (50) or looking at Fig. 4. Therefore, if $\gamma^{(i)}$ is larger than $\hat{\gamma}$, $C^{(i+1)}$ must be larger than $C^{(i)}$ and viceversa. This can be continued with reducing step size until convergence is met.

Once C is computed, B and A can be obtained using Eqs. (49) and (48)

$$B = \sqrt{\frac{\hat{\sigma}^2}{[\Gamma(C_2) - \Gamma^2(C_1)]}} \tag{56}$$

$$A = \hat{\mu} - B\Gamma(C_1) \tag{57}$$

In this way the best fitted Weibull distribution is computed.

Any Stochastic Finite Element Method (SFEM) to be used in conjunction with this fitting procedure must provide for the skewness of the results and compute an accurate value of the third order statistical moment. Small differences in skewness may produce very different curves. The numerical results of Section 4 show that the stochastic approach presented in Section 2 possesses this property and is well suited to be used together with this fitting procedure.

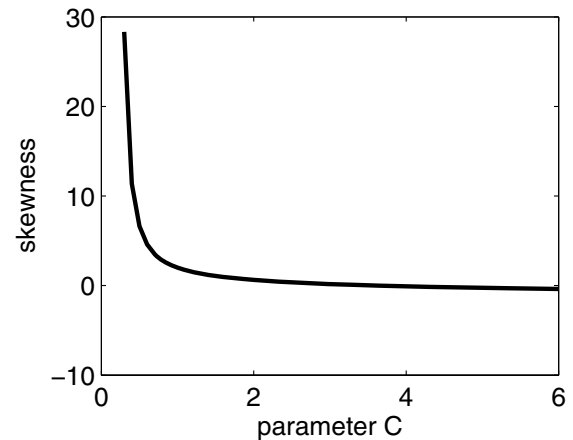


Figure 4 : Strictly decreasing relationship between parameter C and skewness γ .

3.3.2 The Skew-Normal distribution

A new and attractive alternative family of three-parameter distributions is the Skew-Normal (Azzalini, 1985, 1986), which generalizes the standard normal distribution and includes a multivariate version (Azzalini and Dalla Valle, 1996; Azzalini and Capitanio, 1999). This distribution appears well-suited to the present context because it is easy to handle and versatile, as it can assume various symmetric and skew shapes, with a large range of skewness. The standard Skew-Normal is described by the following function:

$$PDF : f(x) = 2\phi(x)\Phi(\vartheta x) \tag{58}$$

where ϑ is the “shape parameter”, ϕ and Φ are, respectively, the standard normal density and cumulative distribution functions (the latter evaluated at point ϑx)

$$\phi(x) = \frac{1}{\sqrt{2\pi}} e^{-\frac{x^2}{2}} \tag{59}$$

$$\Phi(\vartheta x) = \int_{-\infty}^{\vartheta x} \phi(t) dt \tag{60}$$

A generalized Skew-Normal distribution can be obtained using a scale (ω) and a location (ζ) factors. If the random variable X is distributed according to Eq. (58), then the random variable $Y = \zeta + \omega X$ is distributed as a generalized Skew-Normal (SN)

$$Y = \zeta + \omega X \sim SN(\zeta, \omega^2, \vartheta) \tag{61}$$

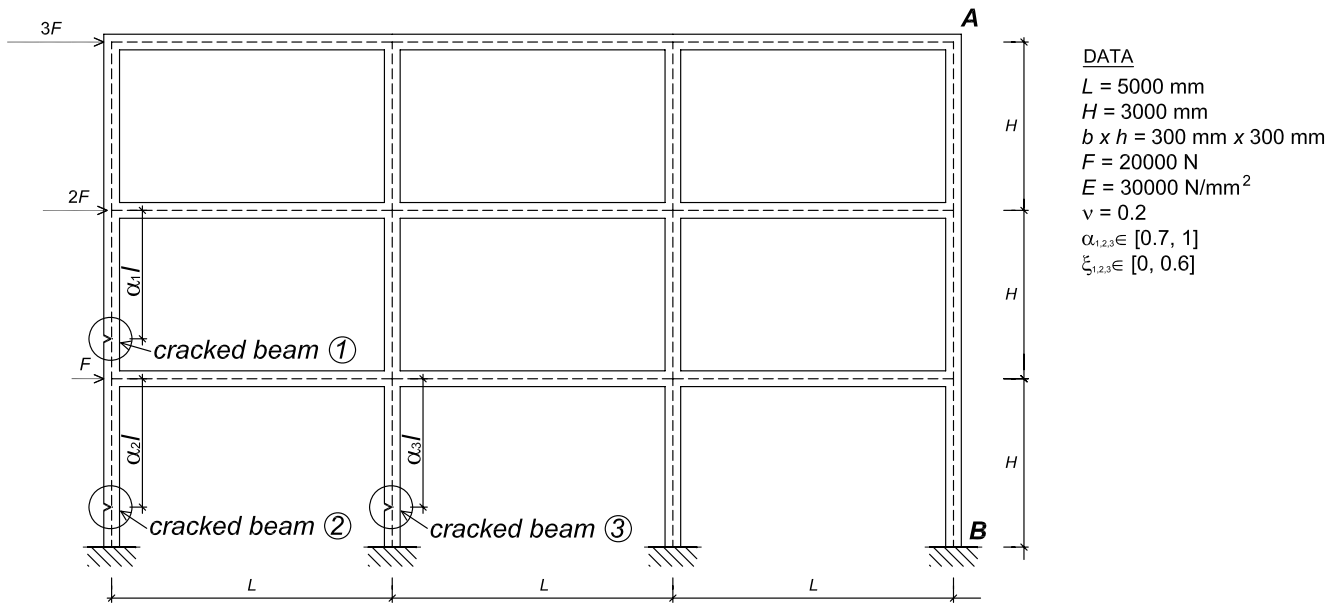


Figure 5 : Multicracked frame structure.

Various procedures can be successfully employed for the estimation of the Skew-Normal distribution. Here, the widely used maximum likelihood method (MLE) is adopted (Beck and Arnold, 1977).

3.4 Minimization of the D_{KS} index

The last approach is based on the index of the Kolmogorov-Smirnov hypothesis test (Benjamin and Cornell, 1970, chap. 4) defined as

$$D_{KS} = \max_x |F(x) - \hat{F}(x)| \quad (62)$$

where $F(x)$ is a theoretical cumulative distribution function and $\hat{F}(x)$ is the empirical cumulative histogram. If a sample of n data x_i is sorted in ascending order, $\hat{F}(x)$ can be computed using the Weibull's formula as

$$\hat{F}(x_i) = \frac{i}{n+1} \quad (63)$$

Here, only the CDF is required to define the theoretical distribution. Therefore, the procedure can be applied in the same way independently of the number of parameters of the assumed distribution.

In other words, for a given sample, D_{KS} is a function of the class of distributions (for example normal, uniform, Skew-Normal, Weibull etc.) and of the parameters of the

distribution. For each class of distributions the set of parameters that minimizes D_{KS} is numerically determined, so specifying a particular curve. Finally, the curve with the overall lowest index is chosen as the result of the fitting procedure.

The minimization of D_{KS} implies a uniform convergence of theoretical and empirical percentiles. If it is applied to SFEMs where random variables characterize single elements, so creating random fields, this method may be interpreted as the imposition of a uniform convergence of iso-probability displacements, stress or strain surfaces.

4 A numerical application

In Fig. 5 a multicracked frame structure with independent and uniformly distributed uncertain parameters (ξ_1, α_1) , (ξ_2, α_2) and (ξ_3, α_3) is represented. The data are shown in the figure. The results are normalized with respect to the solution of the reference configuration. The optimal choice for the reference configuration results in $(\xi_i^0, \alpha_i^0) = (0.51, 0.96)$ for $i = 1, 2, 3$. The predicted distributions for the normalized horizontal displacement at node A and bending moment at node B are reported in Fig. 6. The comparison with classical Monte Carlo simulation evidences the remarkable accuracy of the present approach. In fact, although the high uncertainty level of

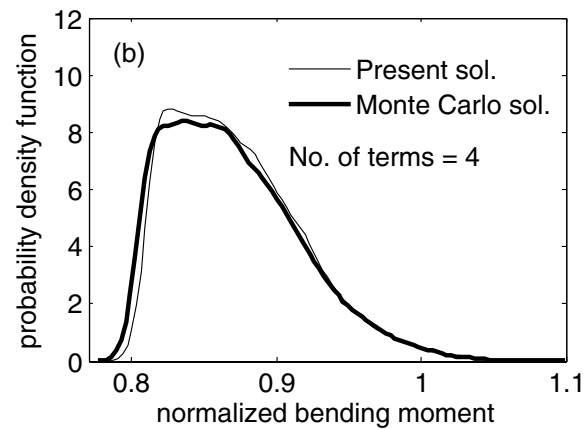
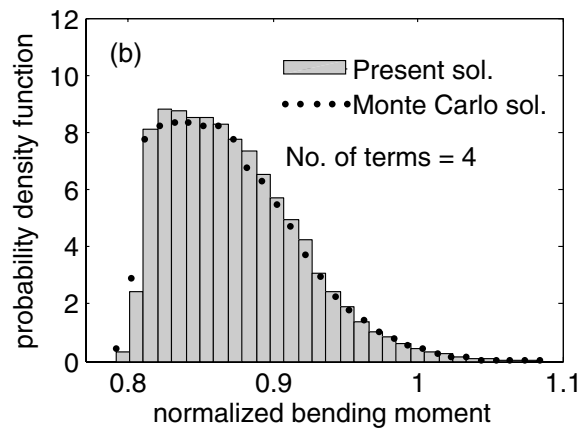
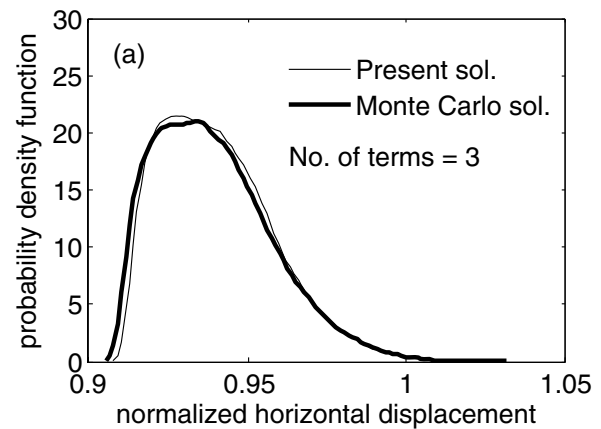
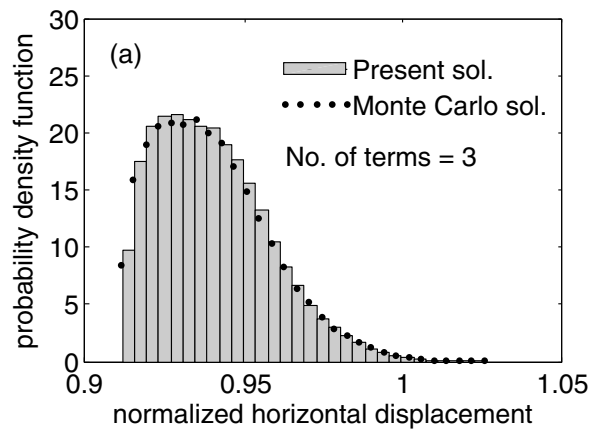


Figure 6 : Relative frequencies of the normalized (a) horizontal displacement at A and (b) bending moment at B.

Figure 7 : Smoothed PDFs of the normalized (a) horizontal displacement at A and (b) bending moment at B.

damage², the structural response is well characterized using few terms for displacements and stresses.

The normalized relative frequency histograms are depicted using only the rough data produced by the stochastic analysis, without any statistical treatment (Section 3.1). As expected, it appears that the representation of the left tail is too poor. However, this approach allows qualitative considerations on the probabilistic characterization of the response. In particular, it shows that both the horizontal displacement at node A and the bending moment at node B are left-skewed. From a structural point of view, designers are interested in the probability of overcoming the upper threshold (area underneath the right tail). Left-skewness implies that, at the right tail,

large ranges of variation of the response determine low probabilities of failure.

A more refined description is obtained by the second approach. The kernel smoothing procedure described in Section 3.2 and applied to the results of Fig. 6 produces the complete curves reported in Fig. 7. Now, an accurate computation of any percentile of the variables becomes trivial.

Figure 8 shows the PDFs obtained by fitting the theoretical distributions. The dashed lines represent the PDFs of the Weibull distributions with parameters estimated by the iterative procedure proposed in Section 3.3.1. The gray lines represent the PDFs of the Skew-Normal distributions with parameters estimated by the maximum likelihood method (MLE). Finally, the theoretical distributions obtained by minimization of D_{KS}

²Note that the interval of variation of the random variable ξ is $[0, 0.6]$.

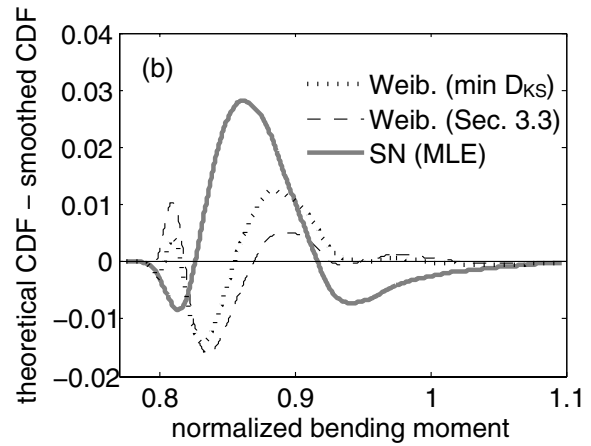
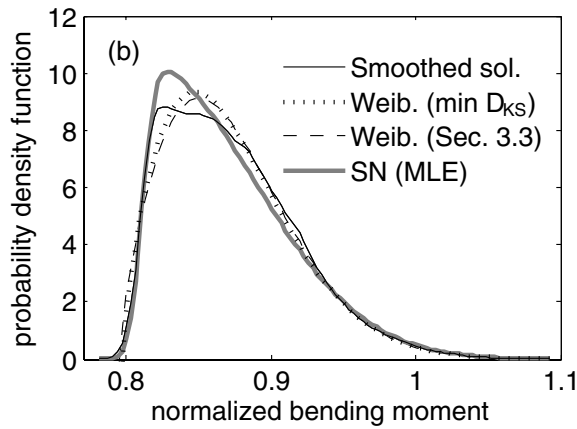
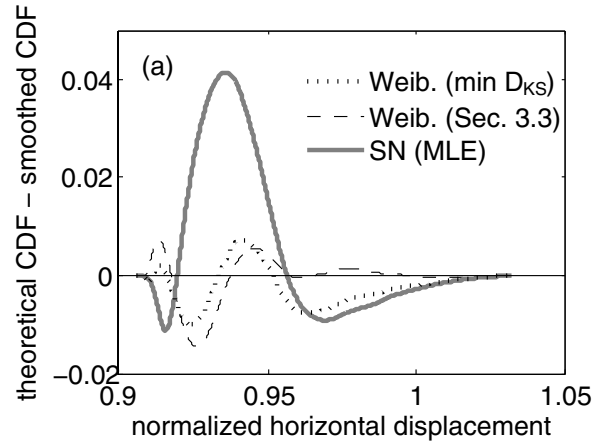
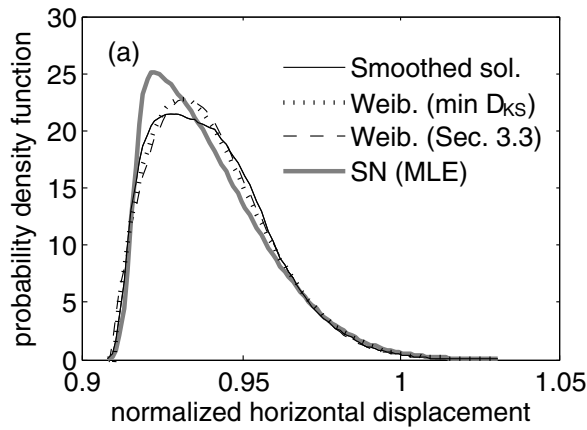


Figure 8 : Theoretical PDFs of the normalized (a) horizontal displacement at A and (b) bending moment at B, fitted by means of the third (Section 3.3) and fourth (Section 3.4) approach.

Figure 9 : Differences on the CDFs of the normalized (a) horizontal displacement at A and (b) bending moment at B between parametric and non-parametric procedures.

are represented by the dotted lines, in both cases they are Weibull distributions. Once the theoretical curve is fitted, the desired quantiles can be easily computed. The fitting performance of the plotted distributions appears evident by considering the Cumulative Distribution Functions (CDFs). The differences among the “smoothed” CDFs and the results of the fitting procedures of the three-parameter distributions (Weibull-Sec.3.3.1 and Skew Normal-MLE) and of the minimization of D_{KS} are compared in Fig. 9. As expected, the latter procedure exhibits rather uniform convergence. Note, however, that also the former procedures yield satisfactory estimates of quantiles near the tails, owing to the versatility of the three-parameter distributions.

In Tables 1 and 2 the Kolmogorov-Smirnov indexes for displacement and bending moment, respectively, have been computed by comparing different approaches. Four two-parameter distributions (uniform, normal, lognormal, Gumbel) have been fitted using the method of moments (Beck and Arnold, 1977). The parameters of the Skew-Normal have been estimated using the maximum likelihood (MLE), while those of the Weibull by the iterative scheme presented in Section 3.3.1. Finally, all the above mentioned distributions have also been fitted by minimizing D_{KS} .

Then, the index of Kolmogorov-Smirnov is used to compare the “goodness of fit” of all the considered probability distributions. The results are collected from the best fitted to the worst one, in the sense of the D_{KS} in-

Table 1 : Kolmogorov-Smirnov indexes for the horizontal displacement at A in ascending order.

Distribution	Parameters	Method	D_{KS}
Weibull	3	min D_{KS}	0.009
Weibull	3	Sec. 3.3.1	0.014
Skew-Normal	3	min D_{KS}	0.018
Gumbel	2	min D_{KS}	0.021
Gumbel	2	moments	0.041
Skew-Normal	3	MLE	0.043
Lognormal	2	min D_{KS}	0.043
Normal	2	min D_{KS}	0.045
Lognormal	2	moments	0.053
Normal	2	moments	0.055
Uniform	2	min D_{KS}	0.500
Uniform	2	moments	1.070

Table 2 : Kolmogorov-Smirnov indexes for the bending moment at B in ascending order.

Distribution	Parameters	Method	D_{KS}
Weibull	3	min D_{KS}	0.013
Skew-Normal	3	min D_{KS}	0.014
Weibull	3	Sec. 3.3.1	0.019
Gumbel	2	min D_{KS}	0.024
Skew-Normal	3	MLE	0.030
Gumbel	2	moments	0.042
Lognormal	2	min D_{KS}	0.044
Normal	2	min D_{KS}	0.048
Lognormal	2	moments	0.055
Normal	2	moments	0.061
Uniform	2	min D_{KS}	0.500
Uniform	2	moments	1.073

dex. As expected, the most accurate results have been obtained using the three-parameter distributions. It appears evident that, in general, the method of moments is less accurate, since it uses only the statistics of the structural response, rather than the whole sample vector. Notice, however, that this feature makes the method applicable also in conjunction with SFEMs that do not provide samples of the response, as, for example, the perturbation method. Moreover, the method proposed in Section 3.3.1 exhibits a good performance, even using only the descriptive statistics of the structural response.

5 Conclusions

A simple, reliable and efficient method for the probabilistic analysis of linear elastic cracked structures with uncertain crack features has been presented. In this paper, the method has been applied to a frame structure with edge cracks of uncertain depth and location. The method has been optimized by a suitable choice of the reference deterministic configuration. The numerical test has revealed a good performance of the present procedure in the case of a multicroaked structure with large fluctuations of damage. In particular, few terms of the series are generally sufficient to accurately characterize the structural response.

The presented stochastic procedure provides not only the descriptive statistics, but also a complete sample of the investigated variables of the structural response. For this reason, it can be used together with all the inference and

fitting methods. In particular, the kernel smoothing techniques, the minimization of the D_{KS} index and the maximum likelihood estimation require a complete sample of the investigated random variables.

The procedure outlined in Section 3.3.1 has been shown to yield a good fit, especially to the tails of the distribution. It should be remarked that this indirectly confirms that the stochastic method accurately captures the skewness of the structural response. On the contrary, the reliability of available Stochastic Finite Element Methods on the evaluation of moments of order higher than two is generally low.

The minimization of the index of Kolmogorov-Smirnov (i) uses the complete information produced by the stochastic procedure, (ii) does not need any *a priori* choice of the class of distributions, (iii) gives very good results in the numerical application and (iv) ensures a uniform convergence. Therefore, in this case it seems to be preferable. The computational effort is higher than that required by other methods, but it is still negligible with respect to the stochastic analysis.

The three-parameter distributions, owing to their versatility, ensure good results regardless of the fitting method. In particular, in the numerical application, the Weibull distribution has provided the best results, but the Skew-Normal seems to be an interesting alternative, with many attractive properties, and worthy of further investigations in the structural reliability framework.

List of symbols

\mathcal{A}	: area of the cross-section
\mathcal{A}_{crack}	: cracked area
A, B, C	: Weibull parameters
b	: width of the rectangular cross-section
\mathbf{C}_a	: compliance matrix
\mathbf{D}_a	: compatibility matrix
\mathbf{D}_a^T	: equilibrium matrix
\mathbf{e}_a	: natural deformations
E	: modulus of elasticity
F	: correction function
G	: shear modulus
h	: height of the rectangular cross-section
I	: indicator function
J	: inertia moment
k	: kernel bandwidth
K	: stress intensity factor
l	: beam length
M	: bending moment
n	: number of data
N	: axial force
\mathbf{q}_a	: natural internal forces
\mathbf{S}_a	: nodal forces
\mathbf{u}_a	: nodal displacements
V	: shear force
w	: kernel function
α	: dimensionless crack position
β_a	: uncertain parameters
γ	: skewness
Γ	: Gamma function
θ	: shape parameter
λ	: compliance
μ, σ^2, γ	: Weibull statistics
$\hat{\mu}, \hat{\sigma}^2, \hat{\gamma}$: Weibull estimators
ν	: Poisson's ratio
ξ	: dimensionless crack depth
ϕ	: standard normal PDF
Φ	: standard normal CDF
ρ	: spectral radius
subscript a	: a^{th} beam element
superscript 0	: deterministic quantity
superscript β	: random quantity

Acknowledgement: This topic is one of the subjects of the Centre of Study and Research for the Identification of

Materials and Structures (CIMEST) “M. Capurso”.

The numerical tests presented were carried out using the facilities of the Laboratory of Computational Mechanics (LAMC) “A. A. Cannarozzi” of the University of Bologna.

References

- Ang, A. H.-S.; Tang, W. H.** (1984): *Probability Concepts in Engineering Planning and Design*. John Wiley and sons, New York.
- Argyris, J. H.; Balmer, H.; Doltsinis, J. S.; Dunne, P. C.; Haase, M.; Kleiber, M.; Malejannakis, G. A.; Mlejnek, H.-P.; Müller, M.; Scharpf, D. W.** (1979): Finite element method - the natural approach. *Computer Methods in Applied Mechanics and Engineering*, vol. 17, pp. 1–106.
- Azzalini, A.** (1985): A class of distributions which includes the normal ones. *Scandinavian Journal of Statistics*, vol. 12, pp. 171–178.
- Azzalini, A.** (1986): Further results on a class of distributions which includes the normal ones. *Statistica*, vol. 46, pp. 199–208.
- Azzalini, A.; Capitanio, A.** (1999): Statistical applications of the multivariate skew normal distribution. *Journal of the Royal Statistical Society: Series B (Statistical Methodology)*, vol. 61, pp. 579–602.
- Azzalini, A.; Dalla Valle, A.** (1996): The multivariate skew-normal distribution. *Biometrika*, vol. 83, pp. 715–726.
- Beck, J. V.; Arnold, K. J.** (1977): *Parameter estimation in engineering and science*. John Wiley and sons, New York.
- Benjamin, J. R.; Cornell, C. A.** (1970): *Probability, statistics and decision for civil engineers*. McGraw-Hill, New York.
- Bocchini, P.; Ubertini, F.; Viola, E.** (2005): An iterative fitting method based on a three-parameter distribution. In Augusti, G.; Schuller, G. I.; Ciampoli, M.(Eds): *Safety and Reliability of Engineering Systems and Structures. Proceedings of the Ninth International Conference on Structural Safety and Reliability*, pp. 2255–2261. Millpress.

- Bowman, A. W.; Azzalini, A.** (1997): *Applied smoothing techniques for data analysis*. Oxford University Press.
- Chou, K. C.; Ingram, E.; Corotis, R. B.** (2005): Optimization approach to the use of goodness-of-fit test. In Augusti, G.; Schuller, G. I.; Ciampoli, M.(Eds): *Safety and Reliability of Engineering Systems and Structures. Proceedings of the Ninth International Conference on Structural Safety and Reliability*, pp. 2201–2208. Millpress.
- Di Paola, M.** (2004): Probabilistic analysis of truss structures with uncertain parameters (virtual distortion method approach). *Probabilistic Engineering Mechanics*, vol. 19, pp. 321–329.
- Epanechnikov, V. A.** (1969): Non-parametric estimation of a multivariate probability density. *Theory of Probability and its Applications*, vol. 14, pp. 153–158.
- Gentilini, C.; Ubertini, F.; Viola, E.** (2005): Probabilistic analysis of linear elastic cracked structures with uncertain damage. *Probabilistic Engineering Mechanics*, vol. 20, pp. 307–323.
- Gentilini, C.; Ubertini, F.; Viola, E.** (2005): Uncertain edge-cracked frame structures. In Aliabadi, M.; Buchholz, F.-G.; Alfaiate, J.; Planas, J.; Abersek, B.; Nishida, S.-I.(Eds): *Proceedings of the fourth International Conference on Fracture and Damage Mechanics*, pp. 371–376.
- Gentilini, C.; Viola, E.; Ubertini, F.** (2003): Probabilistic characterisation of linear truss structures with cracked members. *Key Engineering Materials*, vol. 251-252, pp. 141–146.
- Hurtado, J. E.; Barbat, A. H.** (1998): Monte carlo techniques in computational stochastic mechanics. *Archives of Computational Methods in Engineering*, vol. 5, no. 1, pp. 3–30.
- Matthies, H. G.; Brenner, C. E.; Bucher, C. G.; Soares, C. G.** (1997): Uncertainties in probabilistic numerical analysis of structures and solids-stochastic finite elements. *Structural Safety*, vol. 19, no. 3, pp. 283–336.
- Muller, W.; Herrmann, G.; Gao, H.** (1993): Elementary strength theory of cracked beams. *Theoretical and Applied Fracture Mechanics*, vol. 18, pp. 163–177.
- Murakami, Y.** (1987): *Stress intensity factors handbook*. Pergamon Press, Oxford.
- Nobile, L.** (2000): Mixed mode crack initiation and direction in beams with edge crack. *Theoretical and Applied Fracture Mechanics*, vol. 33, pp. 107–116.
- Okamura, H.; Watanabe, K.; Takano, T.** (1975): Deformation and strength of cracked member under bending moment and axial force. *Engineering Fracture Mechanics*, vol. 7, pp. 531–539.
- Tharp, T.** (1987): A finite element for edge-cracked beam columns. *International Journal for Numerical Methods in Engineering*, vol. 24, pp. 1941–1950.